

δ -function Bose-gas picture of $S=1$ antiferromagnetic quantum spin chains near critical fields

Kouichi Okunishi, Yasuhiro Hieida, and Yasuhiro Akutsu

Department of Physics, Graduate School of Science, Osaka University, Machikaneyama-cho 1-1, Toyonaka, Osaka 560-0043, Japan

(Received 17 July 1998)

We study the zero-temperature magnetization curve ($M-H$ curve) of the one-dimensional quantum antiferromagnet of spin one. The Hamiltonian H we consider is of the bilinear-biquadratic form: $H = \sum_i f(\vec{s}_i \cdot \vec{s}_{i+1})$ (+Zeeman term) where \vec{s}_i is the spin operator at site i and $f(X) = X + \beta X^2$ with $0 \leq \beta < 1$. We focus on validity of the δ -function Bose-gas picture near the two critical fields: upper-critical field H_s above which the magnetization saturates and the lower-critical field H_c associated with the Haldane gap. As for the behavior near H_s , we take ‘‘low-energy effective S matrix’’ approach, where the *correct* effective Bose-gas coupling constant c is extracted from the two down-spin S matrix in its low-energy limit. We find that the resulting value of c differs from the spin-wave value. We draw the $M-H$ curve by using the resultant Bose gas, and compare it with numerical calculation where the product-wave-function renormalization-group (PWFRG) method, a variant of White’s density-matrix renormalization group method, is employed. Excellent agreement is seen between the PWFRG calculation and the correctly mapped Bose-gas calculation. We also test the validity of the Bose-gas picture near the lower-critical field H_c . Comparing the PWFRG-calculated $M-H$ curves with the Bose-gas prediction, we find that there are two distinct regions, I and II, of β separated by a critical value $\beta_c (\approx 0.41)$. In region I, $0 < \beta < \beta_c$, the effective Bose coupling c is positive but rather small. The small value of c makes the ‘‘critical region’’ of the square-root behavior $M \sim \sqrt{H-H_c}$ very narrow. Further, we find that in the $\beta \rightarrow \beta_c - 0$, the square-root behavior transmutes to a different one, $M \sim (H-H_c)^\theta$ with $\theta \approx 1/4$. In region II, $\beta_c < \beta < 1$, the square-root behavior is more pronounced as compared with region I, but the effective coupling c becomes *negative*. [S0163-1829(99)09009-8]

I. INTRODUCTION

The magnetization process ($M-H$ curve, M : magnetization, H : magnetic field) of the one-dimensional (1D) quantum spin system has recently drawn much attention, due to the remarkable progress in material synthesis techniques and high-field experiments.¹ Spin chains with various S (spin magnitude) and/or with nontrivial spatial structures, etc., exhibit various interesting magnetic behaviors (e.g., field-induced phase transitions, like the plateau in the $M-H$ curve²), many of which still await theoretical analyses.

As for the $M-H$ curve of the gapful $S=1$ antiferromagnetic (AF) Heisenberg chain, it has been known that, on raising the magnetic field from zero, there is a critical field H_c above which the system becomes magnetized. This critical field relates to the excitation gap (Haldane gap) Δ as $H_c = \Delta/(g\mu_B)$ (g : g factor, μ_B : Bohr magneton). We call H_c *lower-critical field* because there also exists *upper-critical field* H_s (saturation field) above which the magnetization saturates to $M_s=1$. Near H_s , it is well established that the $M-H$ curve behaves as $M_s - M \sim \sqrt{H_s - H}$.¹³⁻¹⁵ Near H_c , similar behavior $M \sim (H-H_c)^\theta$ with $\theta \approx 1/2$ has also been known,^{7,8} but numerically, whether the exponent θ is *exactly* 1/2 or not, has remained less conclusive as compared with the behavior near H_s .

The expected square-root behavior $M \sim \sqrt{H-H_c}$ has been explained via approximate mapping to the δ -function Bose gas^{7,8} or to the fermion gas.⁹ There is numerical evidence for such mappings,^{8,10} but the square-root behavior of the *bulk magnetization* itself has not been fully verified yet. In the

finite- N (N : system size) diagonalization study,⁸ the smallness of N disables us to make quantitative discussion of the bulk magnetization near H_c . In Ref. 10, a large-size system is treated by the density-matrix renormalization group⁵ (DMRG, for short) to study the low-lying excitations having small $S_{\text{tot}}^z (\leq 4)$. It was shown there that the low-lying excitations admit fermionic interpretation, just as in the case of the Bethe-ansatz solution of the δ -function Bose gas at low-particle density. This result is indeed a strong support for the Bose-gas picture, but the smallness of S_{tot}^z implies that, in a strict sense, the result applies only to the system in the vanishing magnetization density $m = S_{\text{tot}}^z/N \rightarrow 0$.

Further, there is a quantity that is undoubtedly important for the Bose-gas picture, but has not been considered seriously so far: the effective Bose-gas coupling constant c . Let us consider a 1D (effective) δ -function Bose gas with the Hamiltonian

$$\mathcal{H}^{(\text{Bose})}(\sigma, c) = \int dx [\sigma \partial \phi^\dagger(x) \partial \phi(x) + c \phi^\dagger(x) \phi^\dagger(x) \phi(x) \phi(x)], \quad (1.1)$$

with $\phi^\dagger(x)$ and $\phi(x)$ being the Bose operators. By solving the Bethe ansatz integral equation we obtain the ground-state energy density ϵ as¹¹

$$\epsilon = \frac{c^3}{\sigma^2} \tilde{\epsilon}(r), \quad (1.2)$$

$$r = \frac{2\sigma\rho}{c}, \quad \rho: \text{particle number density}, \quad (1.3)$$

$$\tilde{\epsilon}(r) = \frac{\pi^2}{24} r^3 \left\{ 1 - 2r + 3r^2 + \left(\frac{4\pi^2}{15} - 4 \right) r^3 + \left(5 - \frac{4\pi^2}{3} \right) r^4 + \mathcal{O}(r^5) \right\}. \quad (1.4)$$

In terms of the particle density ρ , we have

$$\epsilon(\rho) = A_3 \rho^3 + A_4 \rho^4 + \dots, \quad (1.5)$$

with

$$A_3 = \sigma \pi^2 / 3$$

$$A_4 = -4 \sigma^2 \pi^2 / (3c). \quad (1.6)$$

In the Bose-gas picture, the $M-H$ curve of the spin chain near the critical field corresponds to the $\rho-\mu$ curve of the Bose gas, where $\mu = \partial\epsilon(\rho)/\partial\rho$ is the chemical potential. As far as the critical behavior is concerned, only the ρ^3 term is relevant, which determines both the critical exponent ($=1/2$) and the critical amplitude. Since the coefficient A_3 does not depend on c , the critical behavior must be c independent and ‘‘universal.’’ However, actual $\rho-\mu$ curve heavily depends on the value of c that comes from ρ^4 and/or higher-order terms. In fact, the coefficient A_k of ρ^k term ($k \geq 4$) is proportional to c^{3-k} , which becomes dominant for small c . Accordingly, the critical region of the square-root behavior will become rather narrow for small c . Hence, knowledge of the actual value of the effective coupling constant c is indispensable, in order to make a fully quantitative test of the Bose-gas picture.

The aim of the present article is to give a quantitative test for the Bose-gas picture of the bilinear-biquadratic AF chain in a field. For this purpose, we employ the quantum version³ of the product-wave-function renormalization-group method⁴ (PWFRG method, for short). The PWFRG is a variant of the White’s DMRG,⁵ which is specially designed to obtain the ‘‘fixed point’’ (=thermodynamic limit of the system⁶) of the DMRG iterations efficiently. In Ref. 3, it is shown that the PWFRG, which was originally implemented for 2D classical systems, can also be applied to 1D quantum systems by replacing the transfer-matrix multiplication with the modified Lanczos operation. Even with relatively small number of retained bases, which is conventionally denoted as ‘‘ m ,’’ PWFRG calculations accurately reproduce exact $M-H$ curves for integrable models,^{3,17} which demonstrates both the efficiency and the reliability of the method.

The Hamiltonian of the model we consider is

$$\mathcal{H} = \mathcal{H}_{\text{BLBQ}} - \mathcal{H}_{\text{zeeman}}, \quad (1.7)$$

$$\mathcal{H}_{\text{BLBQ}} = \sum_i [\vec{S}_i \cdot \vec{S}_{i+1} + \beta (\vec{S}_i \cdot \vec{S}_{i+1})^2], \quad \mathcal{H}_{\text{zeeman}} = H \sum_i S_i^z, \quad (1.8)$$

where $\vec{S}_i = (S_i^x, S_i^y, S_i^z)$ is the $S=1$ spin operator at the site i . For notational simplicity, we have taken the units where $g\mu_B = 1$, or, these factors are absorbed into the field H . Note that we have adopted the sign convention where the coeffi-

cient of the biquadratic term is written as $+\beta$, which is different from the one adopted in Ref. 12. In this paper we consider the case $0 \leq \beta < 1$. We concentrate on the behavior of the $M-H$ curve near the two critical fields H_s and H_c .

II. NEAR THE SATURATION FIELD H_s

Let us consider first the system near the upper-critical field (saturation field) $H_s = 4$, where the $M-H$ curve shows the square-root behavior: $1-M \sim \sqrt{H_s - H}$. As compared with the one near H_c , this behavior itself is well-established (by exact diagonalization¹³ and Bethe ansatz^{14,15}). Our concern is how well the δ -function Bose gas can describe the $M-H$ curve away from the saturation field. For this purpose, we should derive the *correct* effective Bose-gas Hamiltonian, which we shall make by employing the low-energy effective S -matrix approach.

Above the saturation field H_s , the system is ferromagnetically ordered (‘‘all-up’’ state). Low-energy excitations slightly below H_s are well described in terms of ‘‘down spins’’ in the sea of up (‘‘+1’’) spins. Regarding a down spin as a particle, we consider two-body scattering problem to obtain the exact two-body S -matrix.^{14,15} The point is that in the *low-energy limit* the S matrix reduces, in most cases, to that of the δ -function Bose gas with an effective coupling constant. With this *correct* coupling constant, the Bose gas will give a quantitative description of the system near H_s .

By $\{|\sigma_1, \sigma_2, \dots, \sigma_N\rangle\}$ ($\sigma_i = 0, \pm 1$), we denote the S^z -diagonal bases of the spin chain. To solve the two-down-spin problem we express the eigenvector $|k, k'\rangle$ in terms of the wave functions $\psi(x, y, k, k')$ and $f(z, k+k')$ as

$$|k, k'\rangle = \sum_{x < y} \psi(x, y, k, k') |1 \cdots 1 \underset{x}{0} 1 \cdots 1 \underset{y}{0} 1 \cdots\rangle \quad (2.1)$$

$$+ \sum_z f(z, k+k') |1 \cdots 1 \underset{z}{(-1)} 1 \cdots\rangle. \quad (2.2)$$

The two-body S -matrix $S(k, k')$ is introduced through the asymptotic ($y-x \rightarrow \infty$) behavior of the wave function

$$\psi(x, y, k, k') \sim e^{ikx} e^{ik'y} + S(k, k') e^{ik'x} e^{iky}. \quad (2.3)$$

The eigenvalue problem $\mathcal{H}_{\text{BLBQ}}|k, k'\rangle = E(k, k')|k, k'\rangle$ is solved to give

$$E(k, k') = \epsilon(k) + \epsilon(k'), \quad (2.4)$$

where $\epsilon(k) = -2 + 2\cos k$ is the one-particle (one-down-spin) energy. Since the one-particle energy $\epsilon(k)$ takes its minimum at $k = \pi$, we put

$$k = \pi + \kappa, k' = \pi + \kappa' \quad (2.5)$$

and consider the ‘‘low-energy limit’’ $\kappa, \kappa' \rightarrow 0$. In this limit, the S matrix whose explicit expression has been given in Ref. 15, becomes

$$S(k, k') \xrightarrow{\kappa, \kappa' \rightarrow 0} S^{(\text{Bose})} \left(\kappa - \kappa', -\frac{3\beta + 1}{\beta} \right), \quad (2.6)$$

where $S^{(\text{Bose})}(k, c)$ is the S matrix of the δ -function Bose gas with Hamiltonian $\mathcal{H}^{(\text{Bose})}(1, c)$ in Eq. (1.1). Explicitly, we have

$$S^{(\text{Bose})}(\kappa, c) = -\frac{c + i\kappa}{c - i\kappa}. \quad (2.7)$$

Therefore, in discussing the low-energy properties near the saturation field, the bilinear-biquadratic chain (1.7) is equivalent to the Bose gas with the effective coupling constant

$$c = -\frac{3\beta + 1}{\beta}. \quad (2.8)$$

Some remarks are in order. For $\beta > 0$ or $\beta < -1/3$ the coupling constant (2.8) takes negative value. It has been known that the δ -function Bose gas with negative coupling constant is unphysical, because the system is unstable against formation of multiparticle bound states. In the present case of finite- S spin chain, however, N -particle bound state with large N are kinematically forbidden because more than $2S$ ‘‘particles’’ cannot exist at a single site; the ‘‘collapse’’ to occur in the negative coupling Bose gas is prevented in the original spin-chain problem. Hence, the effective Bose gas with negative coupling constant, does have a meaning in the present study.

Of course, the above argument based on the ‘‘kinematical constraint’’ on the single-site states does not preclude the existence of N -particle bound states with $N \leq 2S$. Also, there remains possibility of bound states that extend over two or more lattice sites. As for the $S = 1$ bilinear-biquadratic chain, the bound-state problem has been discussed in Ref. 15. The two-particle bound state actually exists, but, for $0 < \beta < 1$ it is a high-energy mode that can be neglected, near the saturation field at least. On the other hand, for $\beta < -1/3$, the lowest-energy excitation mode is actually the two-particle bound state, which modifies the behavior of the $M - H$ curve near the saturation field.¹⁵ In any case, effects of the bound states and the validity of the negative-coupling Bose-gas treatment itself can be tested by a direct numerical calculation of the $M - H$ curve.

We should give another remark concerning the two special points $\beta = 0$ ($c = \infty$) and $\beta = -1/3$ ($c = 0$). The former corresponds to the hard-core Bose gas, which is equivalent to the spinless free-fermion system, and the latter to the free Bose gas. In our Bose-gas mapping scheme based on the low-energy effective S matrix, the above correspondence should be expected only in the low-energy limit (or equivalently, very near the saturation field); the original ‘‘full’’ S matrix $S(k, k')$ actually differs from $S_{\text{free}}(k, k') = \pm 1$ at these special points.¹⁵ To what extent the system behaves as a ‘‘free’’ system is an interesting problem, which can also be studied by a direct numerical calculation.

From the Bose-gas energy density $\epsilon(\rho)$ in Eqs. (1.4) and (1.5) with $\sigma = 1$ and $c = -(3\beta + 1)/\beta$, we obtain the $M - H$ curve through

$$M = 1 - \rho, \quad (2.9)$$

$$H_s - H = \frac{\partial \epsilon(\rho)}{\partial \rho}. \quad (2.10)$$

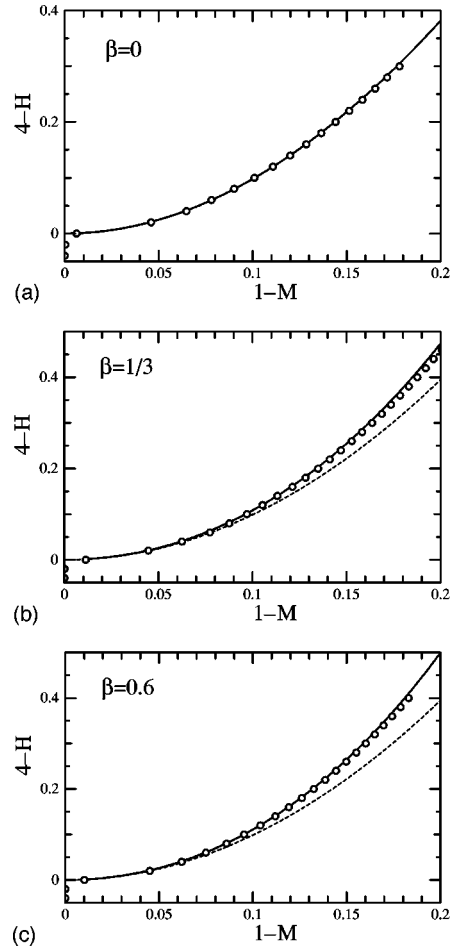


FIG. 1. Comparisons of the effective δ -Bose gas model and the PWFRG calculations near the saturation field H_s for some values of the biquadratic interaction β . (a) $\beta = 0$, (b) $\beta = 1/3$, (c) $\beta = 0.6$. The open circles represent the PWFRG results with the retained number of bases $m = 60$. The solid lines show the effective δ -Bose gas model with the coupling $c = -(3\beta + 1)/\beta$. In (b) and (c), we draw the free fermion curves, which correspond to $|c| = \infty$, as the broken lines for comparison.

At arbitrary ρ , we can numerically solve the Bethe-ansatz integral equation¹¹ by converting it to a matrix equation, to obtain $\partial \epsilon(\rho)/\partial \rho$ within any required precision. To check the validity of the Bose-gas description of the $M - H$ curve, we performed the numerical-renormalization-group calculations. The method we employed is the quantum version³ of the PWFRG,⁴ which allows us to make fixed- H calculations sweeping the value of H giving the $M - H$ curve $M = M(H)$ in the thermodynamic limit. Figure 1 shows comparison between the Bose-gas results and the PWFRG calculations, where we see excellent agreements for unexpectedly wide range of the field H . The validity of the Bose-gas picture in the quantitative description of the $M - H$ curve, is thus verified.

Our two-down-spin S -matrix approach is easily extended to general S bilinear-biquadratic chain with the Hamiltonian

$$\mathcal{H} = \frac{1}{S} \sum_i [\vec{S}_i \cdot \vec{S}_{i+1} + \beta (\vec{S}_i \cdot \vec{S}_{i+1})^2]. \quad (2.11)$$

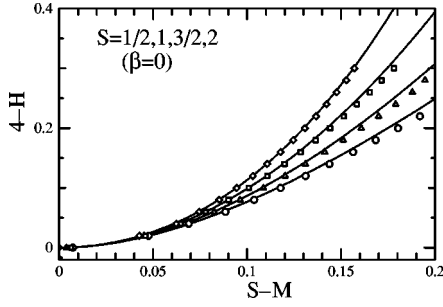


FIG. 2. Comparisons of the effective δ -Bose gas model and the PWFRG calculations for various S at $\beta=0$. The diamonds, squares, triangles, and circles represent the PWFRG results for $S = 1/2, 1, 3/2$, and 2 , respectively. The solid lines represent the effective δ -Bose gas model with $c = 2/(S-1)$.

After a straightforward calculation very similar to the ones in Refs. 14 and 15, we obtain the effective Bose-gas coupling as

$$c = -2 \frac{1 + \beta(3 - 8S + 8S^2)}{1 - S + \beta(3 - 9S + 8S^2)}. \quad (2.12)$$

For the pure bilinear case ($\beta=0$), we have

$$c = 2/(S-1). \quad (2.13)$$

In Fig. 2, we compare the PWFRG-calculated curves for $S = 1/2, 1, 3/2, 2$ to Bose-gas curves with corresponding values of c given by Eq. (2.13). We again see satisfactory agreements.

Let us give a comment on previous studies related to the present one. For the spin- S ‘‘pure’’ Heisenberg AF [$\beta=0$ in Eq. (2.11)], the Bose-gas description near H_s has already been made within the conventional spin-wave theoretical approach.^{18,8} This approach gives the value of the Bose-gas coupling constant to be

$$c = 2/S, \quad (2.14)$$

which is different from Eq. (2.13). The spin-wave value (2.14) deviates from (2.13) very much at small S (even the *sign* disagrees at $S=1/2$), although both are the same in the large S limit. Having seen that the Bose gas with Eq. (2.13) gives the correct $M-H$ curve, we must say that, at small S , the spin-wave approach is not reliable enough for quantitative studies of the AF chains, even in the neighborhood of the saturation field. Note that, using the the Dyson-Maleev transformation and taking the continuum limit, we can formally rewrite⁸ the spin-chain Hamiltonian (2.11) with $\beta=0$ into the δ -function Bose-gas Hamiltonian with Eq. (2.14). Although this transformation seems to be exact in the operator level, there is a constraint on the state space: the boson number cannot exceed $2S$ at each site. This constraint amounts to ‘‘kinematical interaction’’ between the spin waves, which may be the source of the disagreement between Eqs. (2.13) and (2.14).

III. NEAR THE LOWER CRITICAL FIELD H_c

At $H=0$ the ground state is singlet and nonmagnetic. On raising H , system still remains to be singlet up to a critical

field H_c above which the ground-state become magnetized. The field-induced phase transition at H_c is a level-crossing transition between the singlet state and the lowest energy triplet state (both at $H=0$), hence the critical field H_c is, in our unit, just the excitation gap (‘‘Haldane gap’’) Δ . Then, in the Bose-gas description near H_c , the singlet ground state should be interpreted as the ‘‘vacuum,’’ and the triplet state with $S_{\text{tot}}^z = 1$ the ‘‘one-particle state.’’

For $\beta \approx 0$, the ‘‘one-particle’’ energy dispersion $\omega(k)$ takes its minimum at $k = \pi$. The dispersion curve around this minimum is often assumed to be relativistic one,^{19,7}

$$\omega(k) = \sqrt{\Delta^2 + v^2 \bar{k}^2}, \quad (3.1)$$

where $\bar{k} = k - \pi$ and v is called spin-wave velocity. In the low-energy ($|\bar{k}| \rightarrow 0$) limit, Eq. (3.1) becomes

$$\omega(k) = \Delta + \frac{v^2}{2\Delta} \bar{k}^2. \quad (3.2)$$

Unlike the case of $H \approx H_s$, this ‘‘one-particle state’’ cannot be treated exactly, because the ‘‘vacuum’’ itself is not known exactly due to the nonintegrability of the system [except for some special values of β ($= \pm 1, \infty$)]. Accordingly, for general β , it is impossible to calculate the exact two-body S -matrix $S(k, k')$, which is utilized in the previous section to determine the effective coupling constant c . Nevertheless, if we assume the Bose-gas picture to be held, we can ‘‘indirectly’’ determine the value of c from the $M-H$ curve obtained by the PWFRG. To see whether the obtained value of c lies in a reasonable range or not, serves as a partial check of the validity of the Bose-gas picture.

Near $H = H_c = \Delta$, we should relate the $M-H$ curve to the Bose-gas energy density $\epsilon(\rho)$ as

$$M = \rho, \quad H - H_c = \frac{\partial \epsilon(\rho)}{\partial \rho}. \quad (3.3)$$

Then, for the square-root behavior

$$M \sim \sqrt{H - H_c} \quad (H \rightarrow H_c + 0), \quad (3.4)$$

we should expect the expansion of the form,

$$H = H_c + 3A_3 M^2 + 4A_4 M^3 + 5A_5 M^4 + \dots, \quad (3.5)$$

where we have used Eq. (1.5). Since the expression (3.2) of the one-particle energy implies $\sigma = v^2/(2\Delta)$ in Eqs. (1.1) and (1.6), we have

$$A_3 = \frac{\sigma \pi^2}{3} = \frac{\pi^2 v^2}{6\Delta}, \quad (3.6)$$

$$A_4 = -4v^4 \pi^2 / (12\Delta^2 c). \quad (3.7)$$

From Eqs. (1.4)–(1.6), it is clear that the width of critical region essentially depends on the reduced coupling constant \tilde{c} defined by [see Eq. (1.6)]

$$\begin{aligned} \tilde{c} &= c/\sigma, \\ &= -4A_3/A_4. \end{aligned} \quad (3.8)$$

If we rewrite Eq. (3.5) as

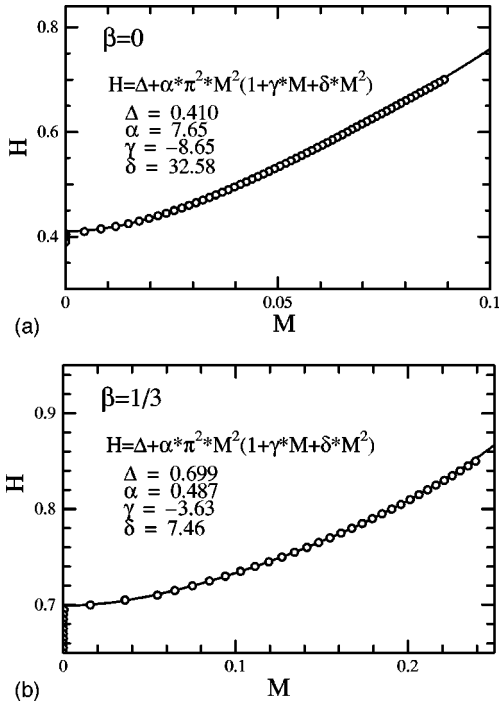


FIG. 3. Comparisons of the effective δ -Bose gas model and the PWFRG calculations near the lower-critical field $H_c(=\Delta)$. (a) The pure AF Heisenberg point $\beta=0$. (b) The AKLT point $\beta=1/3$. The open circles represent the PWFRG results with the retained number of bases $m=100$. The solid lines show the least-square fitting results of the form: $H = \Delta + \alpha \pi^2 M^2 (1 + \gamma M + \delta M^2)$.

$$H - H_c = \alpha \pi^2 M^2 (1 + \gamma M + \delta M^2) [+ O(M^5)], \quad (3.9)$$

a condition for the square-root criticality is $|\gamma M| \ll 1$ (and also $|\delta M| \ll 1$). By $W_M^{(c)}$, we denote width of the critical region in M , which we conveniently define as

$$W_M^{(c)} = 0.1 / |\gamma|. \quad (3.10)$$

Then $M < W_M^{(c)}$ implies $|\gamma M| < 0.1$, which may be regarded as a necessary condition for the criticality. Correspondingly, we can introduce $W_H^{(c)}$ defined by

$$W_H^{(c)} = \alpha \pi^2 (W_M^{(c)})^2, \quad (3.11)$$

which represents the width of the critical region in $H - H_c$.

Let us now check the Bose-gas prediction of the $M - H$ curve by comparing it with the PWFRG calculations. From the $H - M$ curve, we determine $\Delta (= H_c)$, α , γ , and δ in Eq. (3.9) by the least-square fitting. The numerical values for these parameter which we present below are best-fit values. Since DMRG/PWFRG is a deterministic algorithm, hence, our numerical data contain no statistical error, it is hard (and may be meaningless) to estimate the ‘‘error bars.’’ Nevertheless, fitting uncertainty that mainly comes from choice of the ‘‘fitting window’’ (fitting range of M) exists. In this sense, we can make rough estimates of the ‘‘error bars’’ whose typical values are: 1% or less (for Δ), 5% or less (for α), 20% or less (for γ), 50% or less (for δ).

In Fig. 3, we show the PWFRG results of the $H - M$ curves near H_c for $\beta=0, 1/3$. The obtained values of Δ are 0.410 (for $\beta=0$) and 0.699 (for $\beta=1/3$), both of which are

in good agreement with the known values 0.4105 (for the former²⁰) and 0.699 (for the latter^{21,24}).

To verify the relation $\alpha = \sigma = v^2 / (2\Delta)$ we need values of v . For $\beta=0$ using the known value^{10,19} $v=2.46$ we have $\sigma=7.38$, which should be compared with $\alpha=7.65$ obtained from the $H - M$ curve; the obtained value of α is in reasonable agreement with σ . For $\beta=1/3$ there seems to be no serious numerical evaluation of v . We therefore consult Ref. 21 where a variational calculation of $\omega(k)$ beyond the single-mode approximation²² (which gives $\sigma=5/9=0.555\dots$) is made; we have

$$\sigma = (32645 + 359\sqrt{6529}) / 117522 = 0.5246\dots \quad (3.12)$$

This value is also in reasonable agreement with $\alpha=0.487$ obtained from the $H - M$ curve. Hence, the $H - M$ curves reproduce the ‘‘one-particle quantities’’ in the Bose-gas picture.

Although the obtained values of α are consistent with the Bose-gas prediction, the results rely on the fitting form (3.9) (constant + M^2 -term + \dots) whose validity itself should be tested in some way. For this purpose, we replaced the M^2 factor in the second term in the right-hand side of Eq. (3.9) with M^μ , and made the least-square analysis regarding the exponent μ as another fitting variable. As for the $\beta=0$ case, we obtained the best-fit value $\mu=2.01$, which is very close to 2, supporting the expansion (3.9). Hence, in the following analyses, we fix $\mu=2$ and use Eq. (3.9) as the fitting function.

The coefficients γ and δ are estimated to be

$$\beta=0: \gamma = -8.65, \quad \delta = 32.6 \quad (3.13)$$

$$\beta=1/3: \gamma = -3.63, \quad \delta = 7.46. \quad (3.14)$$

Since the negative values of γ implies the positive effective Bose-coupling constant, our PWFRG calculation supports the validity of the Bose-gas picture for $\beta=0, 1/3$.

We should point out that, although the Bose-gas prediction for the square-root behavior seems to be valid, the ‘‘critical region’’ of the square-root behavior in the $M - H$ curve is rather narrow, since the obtained values of γ and δ are non-negligibly large. In fact, the quantity $W_M^{(c)}$ defined by Eq. (3.10) characterizing the width of the critical region, is very small: 0.012 (for $\beta=0$) and 0.028 (for $\beta=1/3$). Corresponding values of $W_H^{(c)}$ defined by (3.11) are even smaller: 0.010 ($\beta=0$) and 3.8×10^{-3} ($\beta=1/3$).

One notable behavior which we found in the PWFRG calculation is that, on raising β from 0, the $H - M$ curve becomes flatter and flatter, or equivalently, the value of α in (3.9) becomes smaller and smaller; there seems to be a critical value $\beta_c (\approx 0.41)$ at which α vanishes. Accordingly, the critical behavior of the $M - H$ curve at H_c changes from square-root type to another one $\sim (H - H_c)^\theta$ ($\theta \approx 0.25$) (Fig. 4). In the Bose-gas picture, this change of the $M - H$ curve may be understood as the vanishing of the \bar{k}^2 term in the expansion of the one-particle excitation energy $\omega(k)$. Interestingly, a qualitative change of the static structure factor $S(q)$ has been found²⁴ very near β_c . Since both of these

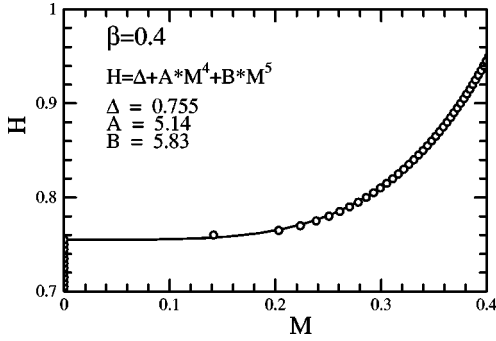


FIG. 4. The $H-M$ curve at $\beta=0.4$ ($\approx\beta_c$) near the lower-critical field $H_c(=\Delta)$. The open circles represent the PWFGR result with $m=100$. The solid line shows the least-square fitting result of the form: $H=\Delta+AM^4+BM^5$.

changes reflect changes in the ground state and the low-energy excitation mode of the system, it is likely that they have a common origin.

The above interpretation for the case of $\beta=\beta_c$ assumes that the system can still be mapped to an interacting Bose gas, although the one-particle energy dispersion $\omega(k)$ may be different from the parabola [$\omega(k)=\Delta+\text{const}\times(\bar{k})^4+\dots$, is expected]. Logically, the breakdown of the Bose-gas mapping itself may also be a possible interpretation. To test whether the system can actually be described by a Bose gas with nonparabolic $\omega(k)$, we should, first of all, know the properties of such “nonparabolic delta-function Bose gas” itself in some detail. However, the nonparabolicity makes the system nonintegrable, disabling us to perform the Bethe ansatz calculation to obtain an exact solution. Nevertheless, we can calculate the two-body S matrix also for the nonparabolic case, and using this, we can apply the “Bethe-ansatz approximation” method^{15,16} to have the low-density behavior of the system. In this view, the M^4 term as the first nontrivial term in the fitting function for $\beta=\beta_c$ can be simply interpreted as the expected \bar{k}^4 term in $\omega(k)$. This line of analysis, which is beyond the scope of the present paper and is left for future study, will help clarify the nature of the bilinear-biquadratic chain at $\beta=\beta_c$.

Above β_c , the square-root behavior reappears. However, the coefficient γ becomes positive (although small), implying *negative* effective coupling constant (Fig. 5). The square-

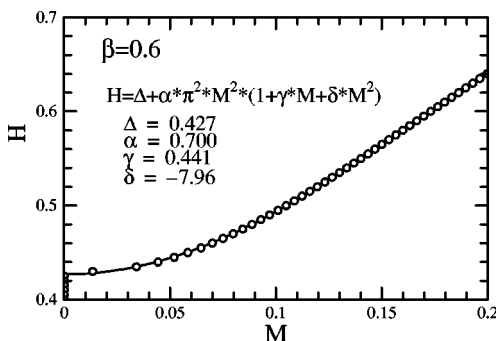


FIG. 5. The $H-M$ curve at $\beta=0.6$ near the lower-critical field $H_c(=\Delta)$. The open circles represent the PWFGR result with $m=100$. The solid line shows the least-square fitting result. We see the Bose-gas coupling constant takes the negative value.

root behavior itself becomes manifest due to small $|\gamma|$, but the negative coupling disables us to take the naive Bose-gas picture in this region of β ; for justification of the picture, we should inspect the “bound states,” just as we did in discussing the $M-H$ curve near the upper-critical field H_s . Note that for systems in the Haldane phase where the orientational order (characterized by the string order parameter²⁵) exists, the “particle” is a moving domain wall separating two regions each of which has complete orientational order.^{26,21,23} In this view, total S^z carried by a low-lying excitation mode is the “height” of the wall. Then, if the wall width is narrow (\sim one lattice spacing), we can adopt a similar reasoning as in the previous section justifying the negative coupling Bose-gas picture: formation of stable bound states will be forbidden due to the kinematical constraint that the local wall height (\sim total S^z , for thin wall) cannot exceed S . The actual situation is, however, subtle because the domain-wall is somewhat fuzzy (due to the zero-spin defects²⁶) and its width may not be narrow.²¹ In this view, we should say that full justification of the Bose-gas picture for $\beta>\beta_c$ seems to require further study. Nevertheless, the square-root behavior $M\sim\sqrt{H-H_c}$ itself is confirmed by our PWFGR calculation.

IV. SUMMARY

In this paper, we have studied the zero-temperature magnetization process ($M-H$ curve) of the $S=1$ isotropic antiferromagnetic spin chain with both the bilinear and biquadratic forms of interactions in the range $0\leq\beta<1$ where β is the coefficient ratio between the biquadratic term and the bilinear term. Quantitative test for the Bose-gas picture near the critical fields H_s (saturation field) and H_c (lower-critical field) has been made with the help of the product-wavefunction renormalization-group (PWFGR) method, which is a variant of White’s density-matrix renormalization group (DMRG).

Near H_s we have derived the correct effective Bose-gas coupling constant from the two down-spin scattering matrix in its low-energy limit. The resulting delta-function Bose gas yields $M-H$ curves, which are in good agreement with the PWFGR calculations.

Near H_c , the square-root behavior $M\sim\sqrt{H-H_c}$ has been confirmed by our PWFGR calculation throughout the range of β studied. Here it should be noted a recent finite-size scaling calculation by Sakai and Takahashi gave a consistent result for the $\beta=0$ case.²⁷ We have, however, found two distinct regions of β separated by a critical value $\beta_c\approx 0.41$. In the small β region, $0<\beta<\beta_c$, the effective Bose-gas coupling c extracted from the PWFGR-calculated $M-H$ curve is positive but small, making the critical region of the square-root behavior rather narrow; it becomes narrower and narrower on approaching β_c . At β_c , the $M-H$ curve seems to exhibit a different critical behavior $M\sim(H-H_c)^\theta$ with $\theta\approx 0.25$. In the large β region, although the square-root behavior is more pronounced due to large value of $|c|$, the sign of c becomes negative, which sharply contrasts to the small- β region.

As regards the $M-H$ curve of the bilinear-biquadratic Heisenberg chain, cusplike singularities in the “middle-field” region have been known for integrable $SU(N)$ chains.²⁸ Whether a similar behavior can also be found for

general, nonintegrable cases is an interesting problem. Although we have concentrated on the behavior near the critical fields in the present paper, we have obtained a full $M-H$ curve from $H=0$ to $H=H_s$. In the large β region, we have actually found a clear cusplike singularity very similar to the one in the $SU(3)$ (Lai-Sutherland) model,²⁹ whose detailed account will be given in a separate paper.

Finally we would like to remark that the Bose-gas description, which we investigated in the present paper may not be the only one for “quantitative” description of the $M-H$ curve of the AF spin chain. For example, in a recent paper, Yamamoto³⁰ gave a different picture for the ground-state properties of the bilinear-biquadratic chain. Such an analysis may be helpful for clarifying nature of the system in the region $\beta > \beta_c$. Also, “quantifying” other low-energy

effective theories is an interesting and important problem. For this purpose, the approach we have taken in Sec. III where microscopic quantities of the effective theory are extracted from bulk quantities calculated by a reliable method, like the DMRG.

ACKNOWLEDGMENTS

The authors would like to thank T. Nishino and H. Kiwata for valuable discussions. This work was partially supported by the Grant-in-Aid for Scientific Research from Ministry of Education, Science, Sports and Culture (No. 09640462). K. O. is supported by JSPS and Y. H. is partly supported by the Sasakawa Scientific Research Grant from The Japan Science Society.

-
- ¹K. Katsumata *et al.*, Phys. Rev. Lett. **63**, 86 (1989); Y. Ajiro *et al.*, *ibid.* **63**, 1424 (1989); T. Takeuchi *et al.*, J. Phys. Soc. Jpn. **61**, 3262 (1992).
- ²K. Hida, J. Phys. Soc. Jpn. **63**, 2359 (1994); S. Sasaki, Phys. Rev. E **53**, 168 (1996); K. Okamoto, Solid State Commun. **98**, 245 (1996); T. Tonegawa, T. Nakao, and M. Kaburagi, J. Phys. Soc. Jpn. **65**, 3317 (1996); K. Totsuka, Phys. Lett. A **228**, 103 (1996); M. Oshikawa, M. Yamanaka, and I. Affleck, Phys. Rev. Lett. **78**, 1984 (1997).
- ³Y. Hieida, K. Okunishi, and Y. Akutsu, Phys. Lett. A **233**, 464 (1997).
- ⁴T. Nishino and K. Okunishi, J. Phys. Soc. Jpn. **64**, 4084 (1995).
- ⁵S. R. White, Phys. Rev. Lett. **69**, 2863 (1992); Phys. Rev. B **48**, 10 345 (1993).
- ⁶S. Östlund and S. Rommer, Phys. Rev. Lett. **75**, 3537 (1995); S. Rommer and S. Östlund, Phys. Rev. B **55**, 2164 (1997).
- ⁷I. Affleck, Phys. Rev. B **43**, 3215 (1991).
- ⁸M. Takahashi and T. Sakai, J. Phys. Soc. Jpn. **60**, 760 (1991).
- ⁹A. M. Tsvelik, Phys. Rev. B **42**, 10 499 (1990).
- ¹⁰E. S. Sørensen and I. Affleck, Phys. Rev. Lett. **71**, 1633 (1993).
- ¹¹E. H. Lieb and W. Liniger, Phys. Rev. **130**, 1605 (1963).
- ¹²I. Affleck, T. Kennedy, E. H. Lieb, and H. Tasaki, Phys. Rev. Lett. **59**, 799 (1987); Commun. Math. Phys. **115**, 477 (1988).
- ¹³J. B. Parkinson and J. C. Bonner, Phys. Rev. B **32**, 4703 (1985).
- ¹⁴R. P. Hodgson and J. B. Parkinson, J. Phys. C **18**, 6385 (1985).
- ¹⁵H. Kiwata and Y. Akutsu, J. Phys. Soc. Jpn. **63**, 3598 (1994).
- ¹⁶W. Krauth, Phys. Rev. B **44**, 9772 (1991).
- ¹⁷R. Sato and Y. Akutsu, J. Phys. Soc. Jpn. **65**, 1885 (1996).
- ¹⁸M. D. Johnson and M. Fowler, Phys. Rev. B **34**, 1728 (1986).
- ¹⁹M. Takahashi, Phys. Rev. B **38**, 5188 (1988); Phys. Rev. Lett. **62**, 2313 (1989); Phys. Rev. B **50**, 3045 (1994).
- ²⁰S. R. White and D. A. Huse, Phys. Rev. B **48**, 3844 (1993); see also Ref. 19.
- ²¹R. Scharf and H.-J. Mikeska, J. Phys.: Condens. Matter **7**, 5083 (1995).
- ²²D. P. Arovas, A. Auerbach, and F. D. M. Haldane, Phys. Rev. Lett. **60**, 531 (1988).
- ²³G. Fáth and J. Sólyom, J. Phys.: Condens. Matter **5**, 8983 (1993).
- ²⁴U. Schollwöck, Th. Jolicœur, and T. Garel, Phys. Rev. B **53**, 3304 (1996).
- ²⁵M. den Nijs and K. Rommelse, Phys. Rev. B **40**, 4709 (1989).
- ²⁶H. Tasaki, Phys. Rev. Lett. **66**, 798 (1991); T. Kennedy and H. Tasaki, Phys. Rev. B **45**, 304 (1992).
- ²⁷T. Sakai and M. Takahashi, Phys. Rev. B **57**, R8091 (1998).
- ²⁸J. B. Parkinson, J. Phys.: Condens. Matter **1**, 6709 (1989); H. Kiwata and Y. Akutsu, J. Phys. Soc. Jpn. **63**, 4269 (1994).
- ²⁹C. K. Lai, J. Math. Phys. **15**, 1675 (1974); B. Sutherland, Phys. Rev. B **12**, 3795 (1975).
- ³⁰S. Yamamoto, Int. J. Mod. Phys. B **12**, 1795 (1998).